

LEGIBILITY NOTICE

A major purpose of the Technical Information Center is to provide the broadest dissemination possible of information contained in DOE's Research and Development Reports to business, industry, the academic community, and federal, state and local governments.

Although a small portion of this report is not reproducible, it is being made available to expedite the availability of information on the research discussed herein.

1990

Los Alamos National Laboratory is operated by the University of California for the United States Department of Energy under contract W 7405 ENG 36

LA-UR--90-2660

DE90 016717

TITLE Order and Chaos in Polarized Nonlinear Optics

AUTHOR(S) Darryl D. Holm

SUBMITTED TO Proceedings of Conference "Chaos Down Under"
Sydney, Australia, Feb. 1990

DISCLAIMER

This report was prepared as an account of work sponsored by an agency of the United States Government. Neither the United States Government nor any agency thereof, nor any of their employees, makes any warranty, express or implied, or assumes any legal liability or responsibility for the accuracy, completeness, or usefulness of any information, apparatus, product, or process disclosed, or represents that its use would not infringe privately owned rights. Reference herein to any specific commercial product, process, or service by trade name, trademark, manufacturer, or otherwise does not necessarily constitute or imply its endorsement, recommendation, or favoring by the United States Government or any agency thereof. The views and opinions of authors expressed herein do not necessarily state or reflect those of the United States Government or any agency thereof.

By acceptance of this article the publisher recognizes that the U.S. Government retains a nonexclusive, royalty-free license to publish or reproduce the copyrighted form of this contribution, or to allow others to do so, for U.S. Government purposes.

This is a preprint of a laboratory report, that the publisher identify this article as work performed under the auspices of the U.S. Department of Energy.

Los Alamos Los Alamos National Laboratory
Los Alamos, New Mexico 87545



ORDER AND CHAOS IN POLARIZED NONLINEAR OPTICS

Darryl D. Holm
Theoretical Division and Center for Nonlinear Studies,
Los Alamos National Laboratory, MS B284
Los Alamos, NM 87545

Abstract

Methods for investigating temporal complexity in Hamiltonian systems are applied to the dynamics of a polarized optical laser beam propagating as a travelling wave in a medium with cubically nonlinear polarizability (i.e., a Kerr medium). The theory of Hamiltonian systems with symmetry is used to study the geometry of phase space for the optical problem, transforming from \mathbb{C}^2 to $\mathbb{S}^2 \times (J, \theta)$, where (J, θ) is a symplectic action-angle pair. The bifurcations of the phase portraits of the Hamiltonian motion on \mathbb{S}^2 are classified and shown graphically. These bifurcations create various saddle connections on \mathbb{S}^2 as either J (the beam intensity), or the optical parameters of the medium are varied. After this bifurcation analysis, the Melnikov method is used to demonstrate analytically that the saddle connections break and intersect transversely in a Poincaré map under spatially periodic perturbations of the optical parameters of the medium. These transverse intersections in the Poincaré map imply intermittent polarization switching with extreme sensitivity to initial conditions characterized by a Smale horseshoe construction for the travelling waves of a polarized optical laser pulse. The resulting chaotic behavior in the form of sensitive dependence on initial conditions may have implications for the control and predictability of nonlinear optical polarization switching in birefringent media.

§1 Introduction

Complexity arising from periodic perturbations of integrable Hamiltonian systems often appears as horseshoe chaos, and is characterized as the limit set of intersections of phase space regions resulting from iterating the Smale horseshoe map. In two-dimensions, the Smale horseshoe map first stretches and folds a rectangular region in phase space into a horseshoe shape of the same area; next the map overlays the horseshoe onto the original rectangle and then takes the intersection. Iterating the horseshoe map repeats this stretching, folding, and intersection process: the two rectangular regions comprising the intersection of the first horseshoe with the original region iterate under the map to make four regions of intersection, iterate again to make eight, and so forth. In the limit, the horseshoe map iterates to produce an invariant Cantor-like set, i.e., a fractal set in phase space called a Smale horseshoe. The dynamics of the horseshoe map on its invariant set can be associated to symbolic shifts. Such shifts produce sensitive dependence on initial conditions, which is the hallmark of chaos. To see intuitively how this sensitive dependence arises, think of each initial condition as the fractional part of a binary number. An iteration of the horseshoe map produces the fractional part of the binary number obtained from the initial one by shifting the "decimal point" one place to the right. Thus, after n iterations the subsequent motion depends on details of the initial condition from beyond its n -th significant figure!

For the periodically perturbed Hamiltonian system considered in this lecture, the Smale horseshoe map is obtained via a Poincaré map, here the time T map of the perturbed phase space orbit, where T is the period of the perturbation. A method due to Melnikov [1963] and Arnold [1964], and developed further by Holmes and Marsden [1982] and Wiggins [1988], is used to establish analytically that iterating the Poincaré map for the perturbed system produces transverse intersections of the stable and unstable manifolds of the perturbed homoclinic points. Each transverse intersection is an unstable homoclinic point of the perturbed Poincaré map and is an unstable periodic orbit of the perturbed system. The Poincaré-Birkhoff-Smale homoclinic theorem is then invoked to assert the existence, near any perturbed transverse homoclinic point, of an invariant Cantor-like set on which some power of the Poincaré map for the perturbed system corresponds to a shift on two symbols, thereby implicating the Smale horseshoe map as the mechanism for chaos. See Wiggins [1988] for explanations and examples of horseshoe chaos, as well as references and discussions concerning the original mathematical development of this field.

In the Melnikov-Arnold method, transverse intersections are shown to exist by establishing for each homoclinic point of the unperturbed system that the (signed) distance in first order perturbation theory between its stable and unstable manifolds develops simple zeroes under

perturbation. (Under small enough perturbations the original homoclinic point displaces slightly, but it continues to exist as a hyperbolic critical point.) Thus, establishing the zeroes of this signed distance (which is usually called the Melnikov function) allows one to conclude that the Poincaré map for the perturbed problem contains the processes of stretching, folding and intersecting necessary to produce an invariant Cantor set under iterations of the map. There are an infinite number of these zeroes of the Melnikov function for the perturbed Poincaré map, and each one corresponds to a transverse intersection of the stable and unstable manifolds of the perturbed homoclinic point. In turn, each of these intersections corresponds to an unstable periodic orbit, around which further transverse intersections can develop in principle, resulting in exquisitely complex dynamics, even for the perturbed Hamiltonian systems in only two dimensions plus time (one and a half degrees of freedom).

For higher degrees of freedom (i.e., in higher dimensions), resonance overlaps and Arnold webs can develop, leading to even richer complexity. While horseshoes and their higher-dimensional counterparts are not strange attractors (since we are dealing only with Hamiltonian systems here), they do have quantifiable mixing and transport properties, and they often behave like strange attractors in numerical simulations (perhaps because of dissipation and noise due to round-off).

The complex dynamics we discuss in this lecture appears in a physical application: the Hamiltonian description of the travelling wave dynamics of a polarized, nearly monochromatic, optical laser pulse propagating in a lossless, cubically nonlinear, parity-invariant, anisotropic, homogeneous medium (for instance, a polarized beam in a straight optical fiber). Our approach combines methods of reduction of phase space dimension for Hamiltonian systems possessing continuous symmetry groups together with the method of Arnold and Melnikov for showing the existence of complex behavior under small perturbations of integrable dynamical systems. This approach provides a unified and geometrical view of the qualitative properties of polarization dynamics (e.g., phase portraits, bifurcations, and special solutions) while at the same time showing that this physical application possesses complex dynamics under conservative spatially-periodic perturbations of the material parameters of the medium.

The plan of the lecture is as follows. In Section 2 we begin by casting the dynamics (Born and Wolf [1986]) of polarized travelling-wave optical pulses into Hamiltonian form, in terms of two complex electric field amplitudes (one amplitude for each linear polarization in the plane transverse to the direction of propagation). Next we use the method of reduction for Hamiltonian systems with symmetry to transform to the Stokes representation of polarization dynamics.

Invariance of the polarization dynamics Hamiltonian under simultaneous changes of phase of the two complex electric field amplitudes leads to conservation of an action variable, J , conjugate to the phase angle, θ . This action variable is the total beam intensity (i.e., the sum of squares of the amplitudes of the two linear polarizations). We perform the reduction process in two steps: from \mathbb{C}^2 to $\mathbb{S}^3 \times \mathbb{S}^1$, first, and then to $\mathbb{S}^2 \times (J, \theta)$. The first reduction gives a geometric picture of the dynamics as taking place along intersections of level surfaces of constants of motion in \mathbb{S}^3 , while the second reduction gives phase portraits on the Poincaré sphere, \mathbb{S}^2 , a level surface of the conserved beam intensity, J . In Section 3 we classify the various fixed points of the reduced dynamics on the Poincaré sphere and describe the bifurcations which take place there as the material parameters and intensity of the light are varied. On this sphere, we find hyperbolic fixed points connected among themselves by homoclinic and heteroclinic orbits. These homoclinic and heteroclinic orbits are separatrices (i.e., stable and unstable manifolds of hyperbolic fixed points) which separate regions on \mathbb{S}^2 having different types of periodic behavior in the travelling-wave frame. For the particular case of a medium whose birefringence is isotropic, we present the complete bifurcation diagram of how these separatrices reconnect among themselves as the beam intensity is varied. In Section 4 we use the Melnikov method to determine that the separatrices tangle and break up into stochastic layers whose Poincaré map is characterized by a Smale horseshoe, under spatially periodic perturbations of the material parameters of the medium. The conclusions of this study are summarized in Section 5.

§2 Hamiltonian Formulation of the Problem

Nonlinear polarization dynamics of optical laser pulses has been studied for about three decades, basically since the invention of the laser. Maker *et al.* [1964] demonstrated the precession of the polarization ellipse for a single beam propagating in a nonlinear medium. Studies of polarization bistability in isotropic media and computer simulations suggesting chaotic behavior can be found in Otsuka *et al.* [1985] and Gaeta *et al.* [1987]. For additional references and more detailed treatments of Hamiltonian chaos in nonlinear optical polarization dynamics see David, Holm and Tratnik [1989a,b,1990].

Propagation of an optical travelling wave pulse in a cubically nonlinear medium is described by the following system of equations (Bloembergen [1965], Shen [1984])

$$i \frac{d}{d\tau} \mathbf{e}_j = \chi_{jk}^{(1)} \mathbf{e}_k + 3\chi_{jklm}^{(3)} \mathbf{e}_k \mathbf{e}_l \mathbf{e}_m^*, \quad (2.1)$$

where τ is the independent variable for travelling waves, $j, k, l, m = 1, 2$, and the complex two-vector $\mathbf{e} = (e_1, e_2)^T \in \mathbb{C}^2$ represents the electric field amplitude. The complex susceptibility tensors $\chi^{(1)}_{jk}$ and $\chi^{(3)}_{jklm}$ parametrize the linear and nonlinear polarizability, respectively. Far from resonance and in a lossless medium, the susceptibility tensors are constant and Hermitian in each $\mathbf{e}-\mathbf{e}^*$ pair and $\chi^{(3)}$ possesses a permutation symmetry:

$$\chi_{jk}^{(1)} = \chi_{kj}^{(1)*}, \quad \chi_{jklm}^{(3)} = \chi_{kjml}^{(3)*}, \quad \chi_{jklm}^{(3)} = \chi_{mklj}^{(3)} = \chi_{jlk m}^{(3)}. \quad (2.2)$$

Hence, we may write the system (2.1) in Hamiltonian form as

$$\begin{aligned} \partial \mathbf{e}_j / \partial \tau &= \{ \mathbf{e}_j, H \}_{\mathbb{C}^2} = -i \partial H / \partial \mathbf{e}_j^*, \\ H &\equiv \mathbf{e}^* \chi_{jk}^{(1)} \mathbf{e}_k + \frac{3}{2} \mathbf{e}^* \mathbf{e}_j \chi_{jklm}^{(3)} \mathbf{e}_k \mathbf{e}_l \mathbf{e}_m^*. \end{aligned} \quad (2.3)$$

In addition, the intensity, $r = |\mathbf{e}|^2 = |e_1|^2 + |e_2|^2$, is conserved. We introduce the three-component Stokes vector, \mathbf{u} , given by (see David, Holm, and Trtnik [1990]) $\mathbf{u} = \mathbf{e}_i^* (\sigma)_{jk} \mathbf{e}_k$, with $\sigma = (\sigma_1, \sigma_2, \sigma_3)$, the standard Pauli matrices. The travelling wave equation (2.1) then becomes

$$\frac{d\mathbf{u}}{d\tau} = (\mathbf{b} + \mathbf{W} \cdot \mathbf{u}) \times \mathbf{u}, \quad \mathbf{b} = \mathbf{a} + |\mathbf{u}| \mathbf{c} = \mathbf{a} + rc, \quad (2.4)$$

where the constant vectors \mathbf{a} and \mathbf{c} , and the constant symmetric tensor \mathbf{W} , are given by

$$\mathbf{a} = (\sigma)_{kj} \chi_{jk}^{(1)}, \quad \mathbf{c} = \frac{3}{2} (\sigma)_{kj} \chi_{jklm}^{(3)}, \quad \mathbf{W} = \frac{3}{2} (\sigma)_{kj} \chi_{iklm}^{(3)} (\sigma)_{lm} = \text{diag}(\lambda_1, \lambda_2, \lambda_3). \quad (2.5)$$

The material parameters \mathbf{a} , \mathbf{c} , and \mathbf{W} are all real. According to equation (2.5), the parameters \mathbf{a} and \mathbf{c} represent the effects of linear and nonlinear anisotropy, respectively. They lead to precession of the Stokes vector \mathbf{u} with (vector) frequency \mathbf{b} . The tensor \mathbf{W} is symmetric, so a polarization basis may always be assumed in which \mathbf{W} is diagonal, $\mathbf{W} = (\lambda_1, \lambda_2, \lambda_3)$, in analogy to the principal moments of inertia of a rigid body.

In terms of the Stokes parameters, \mathbf{u} , the Hamiltonian function H in equation (2.5) may be rewritten as

$$H = \mathbf{b} \cdot \mathbf{u} + \frac{1}{2} \mathbf{u} \cdot \mathbf{W} \cdot \mathbf{u} \quad (2.6)$$

and the equations of motion (2.9) may be expressed in Hamiltonian form as $du/d\tau = \{\mathbf{u}, H\}$, by using the Lie-Poisson bracket $\{F, G\} := \mathbf{u} \cdot \nabla F(\mathbf{u}) \times \nabla G(\mathbf{u})$ written in triple scalar product form, just as in the case of the rigid body. The intensity $r = |\mathbf{u}|$ is the Casimir function for this Lie-Poisson bracket. That is, the intensity r Poisson-commutes with all functions of \mathbf{u} when the above Lie-Poisson bracket is used; so r in the Stokes description of lossless polarized optical beam dynamics may be regarded simply as a constant parameter. (See Holm, *et al.* [1985], for discussions and references concerning Lie-Poisson brackets and their usage, for example, in the study of Lyapunov stability of equilibrium solutions of dynamical systems.)

Solving the system (2.4) when (a) two eigenvalues of \mathbf{W} coincide, and (b) one or more of the components of \mathbf{b} vanish, can be done easily for two cases which are inequivalent under cyclic permutations of indices of \mathbf{u} . In the first case, we set $\mathbf{W} = \omega \text{diag}(1, 1, 2)$ and $\mathbf{b} = (b_1, b_2, 0)$; equations (2.4) then read

$$du_1/d\tau = (b_2 - \omega u_2)u_3, \quad du_2/d\tau = (\omega u_1 - b_1)u_3, \quad du_3/d\tau = b_1 u_2 - b_2 u_1. \quad (2.7)$$

Hence, a Duffing equation emerges for u_3 ,

$$d^2 u_3/d\tau^2 = A u_3 (B - u_3^2), \quad (2.8)$$

$$A = \frac{1}{2} \omega^2, \quad B = \frac{2H}{\omega} - r^2 - \frac{2(b_1^2 + b_2^2)}{\omega^2}.$$

The other two components of \mathbf{u} may be determined algebraically from the two constants of motion r and H . When B increases through zero, the Duffing equation (2.8) develops a pair of orbits, homoclinic to the fixed point u_3 (see, e.g., Guckenheimer and Holmes [1983] and Wiggins [1988]). Likewise, in the second case, we set $\mathbf{W} = \omega \text{diag}(1, 1, 2)$ and $\mathbf{b} = (b_1, 0, b_3)$; equations (2.4) then become

$$du_1/d\tau = -b_3u_2 - \omega u_2u_3, \quad du_2/d\tau = \omega u_1u_3 + b_3u_1 - b_1u_3, \quad du_3/d\tau = b_1u_2. \quad (2.9)$$

Hence, provided $b_1 \neq 0$, we find

$$d^2u_3/d\tau^2 = A' + B'u_3 + C'u_3^2 + D'u_3^3, \\ A' = b_3(H - \frac{1}{2}\omega r^2), \quad B' = \omega H - \frac{1}{2}\omega^2 r^2 - b_1^2 - b_3^2, \quad C' = -\frac{3}{2}\omega b_3, \quad D' = -\frac{1}{2}\omega^2. \quad (2.10)$$

Thus, the polarization dynamics for this case reduces to the motion of a particle in a quartic potential, whose solution is expressible in terms of elliptic integrals. Again, the components u_1 and u_2 may be determined algebraically from the two constants of motion, r and H . We shall return to these two cases later, when we discuss the effects of perturbations. For now, these cases suffice to demonstrate that the system (2.4) possesses bifurcations in which homoclinic orbits are created.

The system of equations (2.9) further reduces the Poincaré sphere Σ_r of radius r upon transforming to spherical coordinates $(u_1, u_2, u_3) = (r\sin\theta\sin\varphi, r\cos\theta, r\sin\theta\cos\varphi)$. In these coordinates, the reduced Hamiltonian function (2.6) and the symplectic Poisson bracket on Σ_r are expressible as

$$H = \frac{1}{2}r^2[(\lambda_1\sin^2\varphi + \lambda_3\cos^2\varphi)\sin^2\theta + \lambda_2\cos^2\theta] + r\sin\theta(b_1\sin\varphi + b_3\cos\varphi) + b_2r\cos\theta, \\ \{F, G\} := \frac{1}{r} \frac{\partial F}{\partial \varphi} \frac{\partial G}{\partial \cos\theta} - \frac{1}{r} \frac{\partial G}{\partial \varphi} \frac{\partial F}{\partial \cos\theta}. \quad (2.11)$$

and the equations of motion are

$$d\theta/d\tau = b_1\cos\varphi - b_3\sin\varphi + (\lambda_1 - \lambda_3)r\sin\theta\cos\varphi\sin\varphi, \\ d\varphi/d\tau = b_2 - (b_1\sin\varphi + b_3\cos\varphi)\cot\theta - r(\lambda_1\sin^2\varphi + \lambda_3\cos^2\varphi - \lambda_2)\cos\theta. \quad (2.12)$$

The system (2.9) is completely integrable, since it is a one-degree-of-freedom Hamiltonian system. Its solutions are expressible in terms of elliptic integrals.

§3 Bifurcation analysis

We now specialize to the case of a non-parity-invariant material with C_4 rotation symmetry about the axis of propagation (the z-axis), for which material constants take the form $\mathbf{W} = (\lambda_1, \lambda_2, \lambda_3)$ and $\mathbf{b} = (0, b_2, 0)$. (See David, Holm, and Tratnik [1990] for details of what follows.) We also introduce the following parameters

$$\mu = \lambda_3 - \lambda_1, \quad \lambda = (\lambda_2 - \lambda_1)/(\lambda_3 - \lambda_1), \quad \beta = b_2/[r(\lambda_3 - \lambda_1)]. \quad (3.1)$$

In this case, the Hamiltonian in (2.11) and the equations of motion become

$$H = \frac{1}{2}\mu[(r^2 - u^2)\cos^2\varphi + \lambda u^2 + 2\beta ru] + \frac{1}{2}\lambda_1 r^2, \quad (3.2a)$$

$$du/d\tau = \mu(r^2 - u^2)\cos\varphi\sin\varphi, \quad (3.2b)$$

$$d\varphi/d\tau = \mu[\beta r - (\cos^2\varphi - \lambda)u], \quad (3.2c)$$

where $u \equiv r\cos\theta$. We construct the phase portrait of the system and explain how this portrait changes as the parameters in the equations vary. The fixed points of (3.2b, c) are easily located and classified, using standard techniques. We list them in the Table, for $\mu \neq 0$. The special case where $\mu = 0$, i.e., $\lambda_3 = \lambda_1$, requires a separate analysis. In that case, the right-hand side of (1.4a) vanishes identically so that the set of fixed points of the system is the circle $\cos\theta = b_2/r(\lambda_2 - \lambda_1) = \beta/\lambda$. The phase portrait depends on two essential parameters, λ and β , or equivalently, $\lambda_2 - \lambda_1$ and b_2/r . Bifurcations of the phase portrait occur when the inequality constraints in the third column of the Table become equalities; hence we observe that the pairs of fixed points (F, B) and (L, R) appear or vanish as the lines $\beta = \pm(1 - \lambda)$ and $\beta = \pm\lambda$ are crossed in the (λ, β) parameter plane (see Figure 1).

Fixed Point	Coordinates	Constraint	Saddle	Center
F	$\varphi = 0 \quad \cos\theta = \beta/(1 - \lambda)$	$\beta^2 < (1 - \lambda)^2$	$\lambda > 1$	$\lambda < 1$
B	$\varphi = \pi \quad \cos\theta = \beta/(1 - \lambda)$			
L	$\varphi = \pi/2 \quad \cos\theta = \beta/\lambda$	$\beta^2 < \lambda^2$	$\lambda < 0$	$\lambda > 0$
R	$\varphi = -\pi/2 \quad \cos\theta = \beta/\lambda$			
N	$\cos^2\varphi = \lambda + \beta \quad \theta = 0$	—	$\beta \in (-\lambda, 1 - \lambda)$	$\beta \in (-\lambda, 1 - \lambda)$
S	$\cos^2\varphi = \lambda - \beta \quad \theta = \pi$	—	$\beta \in (\lambda - 1, \lambda)$	$\beta \in (\lambda - 1, \lambda)$

Table. The fixed points of system (3.2) and their types.

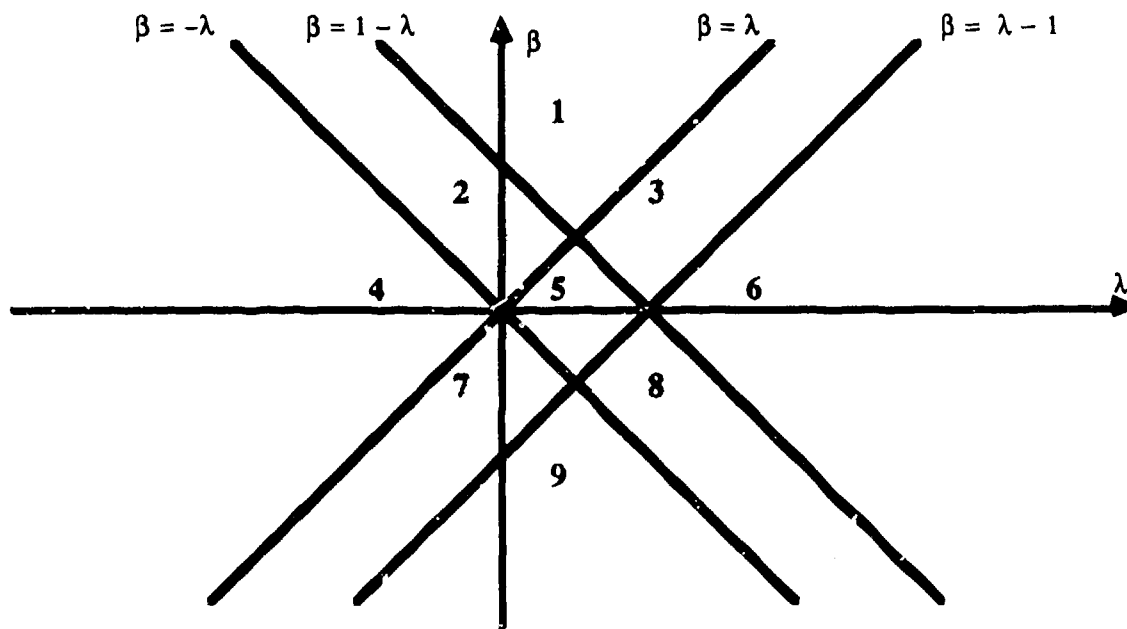


Figure 1. The parameter plane and its bifurcation lines.

The (λ, β) parameter plane is partitioned into nine distinct regions separated by four critical lines that intersect in pairs at four points. Typical phase portraits corresponding to each of these regions are shown in Figure 2. Note that the phase portraits of the unperturbed system (3.2b,c) are invariant under the following discrete transformations:

$$\begin{array}{ll} \varphi \rightarrow \varphi \pm \pi; & \varphi \rightarrow \varphi \pm \pi, \theta \rightarrow \pi - \theta, \beta \rightarrow -\beta; \\ \varphi \rightarrow \varphi \pm \pi/2, \lambda \rightarrow 1 - \lambda, \beta \rightarrow -\beta; & \varphi \rightarrow \varphi \pm \pi/2, \lambda \rightarrow 1 - \lambda, \theta \rightarrow \pi - \theta. \end{array}$$

Thus, as far as the configurations of critical orbits on the phase sphere are concerned, it will be sufficient to consider the quarter plane given by $\lambda < 1/2$ and $\beta > 0$, i.e., to restrict attention to regions 1, 2, 4, and 5. Although no bifurcations occur when the λ -axis ($\beta = 0$ in the parameter plane) is crossed (except for $\lambda = 0$, and $\lambda = 1$, the set of fixed points does not change), this line is nevertheless special. Indeed, in the interval $\lambda \in (0, 1)$, i.e. within region R5, both poles are hyperbolic, each one of them being attached to a pair of homoclinic loops. When β vanishes, these homoclinic loops merge together so as to form four heteroclinic lines (and thus four heteroclinic 2-cycles) connecting the north and south poles together. On the λ -axis the polarization dynamics reduces to that of the rigid body. In that case, the phase portrait consists of the poles N and S, and the four other points are located on the equator of S^2 (this configuration of fixed points distributed on the equator is obtained only on this line). Two of these, (N, S) or (F, B) or (R, L), are unstable while the other four are stable; which pair is unstable is decided by the value of $\lambda = (\lambda_2 - \lambda_1)/(\lambda_3 - \lambda_1)$. The pair (F, B) is hyperbolic when $\lambda < 0$, (N, S) are hyperbolic when $0 < \lambda < 1$, and (R, L) are hyperbolic whenever $\lambda > 1$; in each of these cases, the unstable direction is specified by the λ_i which is neither the least nor the greatest among the three.

Bifurcations taking place as the beam intensity is varied are those occurring along a vertical line in the parameter plane; we present a list of the seven possible sequences (See David, Holm, and Tratnik [1990] for an exhaustive list of the bifurcations that may take place in the phase phase when travelling along these lines):

$S_1:$	$\lambda < 0$	$R1 \leftrightarrow R2 \leftrightarrow R4 \leftrightarrow R7 \leftrightarrow R9$
$S_2:$	$\lambda = 0$	$R1 \leftrightarrow R2 \leftrightarrow R7 \leftrightarrow R9$
$S_3:$	$0 < \lambda < 1/2$	$R1 \leftrightarrow R2 \leftrightarrow R5 \leftrightarrow R7 \leftrightarrow R9$
$S_4:$	$\lambda = 1/2$	$R1 \leftrightarrow R5 \leftrightarrow R9$
$S_5:$	$1/2 < \lambda < 1$	$R1 \leftrightarrow R3 \leftrightarrow R5 \leftrightarrow R8 \leftrightarrow R9$
$S_6:$	$\lambda = 1$	$R1 \leftrightarrow R3 \leftrightarrow R8 \leftrightarrow R9$
$S_7:$	$\lambda > 1$	$R1 \leftrightarrow R3 \leftrightarrow R6 \leftrightarrow R8 \leftrightarrow R9$

§4 *Homoclinic chaos.*

In this section, we consider spatially periodic modulations of either the circular-circular polarization self-interaction coefficient λ_2 in W or the optical activity b_2 . In each case, when the unperturbed medium satisfies the additional condition $\lambda_2 = \lambda_3$, the Melnikov technique (Melnikov [1963], Guckenheimer and Holmes [1983] and Wiggins [1988]) leads to an analytically manageable integral for the Melnikov function, which is shown to have simple zeros. In this way, horseshoe chaos is predicted in the dynamics of the single Stokes pulse. We also discuss the physical implications for measuring this horseshoe chaos in an experimental situation.

We concentrate on the north pole $u_2 = 1$, $\varphi = \varphi_0$, with $\cos^2 \varphi_0 = \lambda + \beta$, and evaluate the conserved Hamiltonian at this point to find a relation between u and φ on the homoclinic orbit,

$$u_2 = -r - 2b_2/\mu(\cos^2 \varphi - \lambda), \quad (4.1)$$

which, when substituted into the equation of motion for φ , gives

$$d\varphi/d\tau = \mu r(\cos^2 \varphi - \cos^2 \varphi_0). \quad (4.2)$$

Upon integrating (4.2) we obtain (with $\tau = z + vt$, the travelling-wave variable)

$$\tan\varphi = \tan\varphi_0/\tanh(\zeta\tau), \quad \zeta = \frac{1}{2}\mu r \sin(2\varphi_0). \quad (4.3)$$

Substituting this formula into (4.1) gives an analytical expression for u on the homoclinic orbit:

$$u_2 = -r - \frac{2b_2[1 - \cos^2\varphi_0 \operatorname{sech}^2(\zeta\tau)]}{\mu\{\cos^2\varphi_0 \tanh^2(\zeta\tau) - \lambda[1 - \cos^2\varphi_0 \operatorname{sech}^2(\zeta\tau)]\}}. \quad (4.4)$$

We consider a periodic perturbation of the eigenvalue λ_2 and the optical activity b_2 , that is,

$$\hat{\lambda}_2' = \lambda_2 + \varepsilon_1 \cos(\nu z), \quad b_2' = b_2 + \varepsilon_2 \cos(\nu z), \quad (4.5)$$

where $\varepsilon_{1,2} \ll 1$ and ν is the modulation frequency. Then from (2.6) the perturbation Hamiltonian is

$$H^1 = \frac{1}{2} u_2 (\varepsilon_1 u_2 + 2\varepsilon_2) \cos(\nu z), \quad (4.6)$$

and we easily calculate the Poisson bracket of this perturbation with the unperturbed Hamiltonian:

$$\{H^0, H^1\} = -\mu \sin\varphi \cos\varphi (r^2 - u^2) u_2 \cos(\nu z), \quad (4.7)$$

which when formally integrated becomes the Melnikov function

$$M(\tau_0) = \mu \int_{\mathbb{R}} \sin\varphi(\tau) \cos\varphi(\tau) [r^2 - u^2(\tau)] (\varepsilon_1 u_2 + \varepsilon_2) \cos[\nu(\tau - \tau_0)] d\tau, \quad (4.8)$$

where $\tau_0 = \nu t$. In the particular case $\lambda_2 = \lambda_3$, this integrable is manageable and can be found in standard tables. Hence,

$$M(\tau_0) = \frac{2\pi v^2}{b_2^2} \left[r(\epsilon_1 r + \epsilon_2) + \frac{2}{3} \epsilon_1 r^2 [\cos^2 \varphi_0 + (v/2b_2)^2] \right] \text{csch}[v\pi/\mu r \sin(2\varphi_0)] \sin(v\tau_0), \quad (4.9)$$

which clearly has simple zeros as a function of τ_0 , implying horseshoe chaos (see, e.g., Guckenheimer and Holmes [1983] and Wiggins [1988]). When the Melnikov function has simple zeros, the dynamical evolution of a rectangular region near the homoclinic point shows (under iteration of the Poincaré map induced from the periodic perturbation) that the region is folded, stretched, contracted, and eventually mapped back over itself in the shape of a horseshoe. This horseshoe map is the underlying mechanism for chaos. As the horseshoe folds and refolds, the rectangular region of phase points initially lying near the homoclinic point develops a Cantor set structure whose associated Poincaré Map can be shown to contain countably many unstable periodic motions, and uncountably many unstable nonperiodic motions. (See Guckenheimer and Holmes [1983] and Wiggins [1988] for the methods of proof of these statements and further descriptions of homoclinic tangles.)

§5 Conclusions.

Physically, the horseshoe chaos in the case of a periodically perturbed single Stokes pulse corresponds to intermittent switching from one elliptical polarization state, to another one whose semimajor axis is approximately orthogonal to that of the first state, with a passage close to the unstable circular polarization state during each switch. This intermittency is realized on the Poincaré sphere by an orbit which spends most of its time near the unperturbed *figure eight* shape with a (homoclinic) crossing at the north pole (circular polarization) in Figure 2. Under periodic perturbations of either the W -eigenvalues or the optical activity b_2 , this orbit switches deterministically, but with extreme sensitivity to the initial conditions, from one lobe of the figure eight to the other each time it returns to the crossing region near the north pole where the homoclinic tangle is located. Thus, for the one-beam problem we predict intermittent and practically unpredictable switching under spatially periodic perturbations of the material parameters, as the optical polarization state passes through a homoclinic tangle near the circular polarization state.

From considerations of the special case in which the Duffing equation (2.8) appears, one could have expected homoclinic chaos to develop for nonlinear optical polarization dynamics.

Indeed, a related special case is studied numerically in Wabnitz [1987]. As opposed to such numerical studies, our analytical treatment explores the bifurcations available to the polarization dynamics under the full range of material parameter variations, demonstrates that the horseshoe construct is the mechanism driving the chaotic behavior, and characterizes the location of the chaotic set, or stochastic layer, and the dependence of its width on the material parameters, modulation frequency, and optical beam intensity.

In the cases under consideration, this stochastic layer is bounded by KAM (Kolmogorov-Arnold-Moser) curves on the Poincaré sphere, inside of which the travelling-wave dynamics is regular and orbitally stable. For a given choice of beam and material parameters, these KAM curves define phase space regions where chaotic behavior (for example, sensitive dependence on initial conditions, or orbital instability) may be found, and complementary regions where chaos is absent and only regular, predictable behavior may be found.

The strong dependence on intensity of the phase-space portraits reported here indicates that control and predictability of optical polarization in nonlinear media may become an important issue for future research. In particular, the sensitive dependence on initial conditions in nonlinear polarization dynamics found here to be induced by spatial inhomogeneities may have implications for the control and predictability of optical polarization switching in birefringent media. For instance, an input-output polarization experiment performed with input conditions lying in the stochastic layer for some set of material and beam parameters will show essentially random output after sufficient propagation length, depending on the amplitude and wavelength of the material inhomogeneities and the type of (transparent) material used for the experiment.

While in Australia, the author learned from D.J. Mitchell and A. W. Snyder that the equations studied here also apply to nonlinear directional couplers (Snyder and Love [1983]), and that recent experiments in these couplers also show the sensitive intermittent switching effect explained here in terms of Smale horseshoe dynamics. See also Snyder *et al.* [1990].

Acknowledgments. The work reported here was done in collaboration with D. David and M. Tratnik at Los Alamos National Laboratory. We thank S. Wiggins, A.V. Mikhailov and Y. Kodama for stimulating scientific discussions during the course of this work. The author thanks N. Joshi and A. Oppie for their hospitality at The Australian National University and The University of New South Wales. He also thanks J. Monaghan for his hospitality at Monash University.

References.

V.I. Arnold [1964]. Instability of dynamical systems with several degrees of freedom, *Sov. Math. - Dokl.* **5**, 581-585.

N. Bloembergen [1965]. *Nonlinear Optics*, Benjamin: New York.

M. Born and E. Wolf [1986], *Principles of Optics*, Sixth edition, Pergamon Press: Oxford.

D. David, D.D. Holm, and M.V. Tratnik [1989a]. Integrable and chaotic polarization dynamics in nonlinear optical beams, *Phys. Lett A* **137**, 355-364.

D. David, D.D. Holm, and M.V. Tratnik [1989b]. Horseshoe chaos in a periodically perturbed polarized optical beam, *Phys. Lett A* **138**, 29-36.

D. David, D.D. Holm, and M.V. Tratnik [1990]. Hamiltonian chaos in nonlinear optical polarization dynamics, *Phys. Rep.* **187**, 282-367.

A.L. Gaeta, R.W. Boyd, J.R. Ackerhalt and P. Milonni [1987]. Instabilities and chaos in the polarizations of counterpropagating light fields, *Phys. Rev. Lett.* **58**, 2432-2435.

J. Guckenheimer and P. Holmes [1983]. *Nonlinear Oscillations, Dynamical Systems, and Bifurcations of Vector Fields*, Springer-Verlag: New York.

D.D. Holm, J.E. Marsden, T. Ratiu, and A. Weinstein [1985]. Nonlinear stability of fluid and plasma equilibria, *Physics Reports* **123**, 1-116.

Holmes and Marsden [1982]. Mel'nikov's method and Arnold diffusion for perturbations of integrable Hamiltonian systems, *J. Math. Phys.* **23**, 669-675.

P.D. Maker, R.W. Terhune, and C.M. Savage [1964]. Intensity-dependent changes in the refractive index of liquids, *Phys. Rev. Lett.* **12**, 507-509.

V.K. Melnikov [1963]. On the stability of the center for time periodic perturbations, *Trans. Moscow Math. Soc.* **12**, 1-57.

K. Otsuka, J. Yumoto, and J.J. Song [1985]. Optical bistability based on self-induced polarization-state change in anisotropic Kerr-like media, *Opt. Lett.* **10**, 508-510.

Y.R. Shen [1984]. *The Principles of Nonlinear Optics*, Wiley-Interscience: New York.

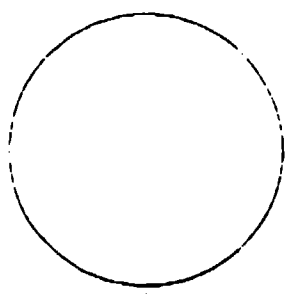
A.W. Snyder and J.D. Love [1983]. *Optical Waveguide Theory*, Chapman & Hall: London.

A.W. Snyder, D.J. Mitchell, Y. Chen, L. Poladian and D. Rowland [1990]. Nonlinear fiber amplifiers and switches: order and chaos, submitted to *J. Opt. Soc. Am. B*.

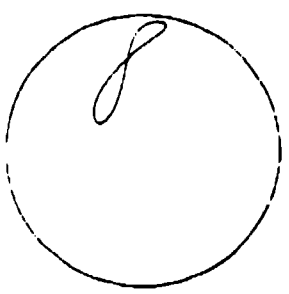
S. Trillo S. Wabnitz, and R.H. Stolen [1986]. Experimental observation of polarization instability in a birefringent optical fiber, *Appl. Phys. Lett.* **49**, 1224-1226.

S. Wabnitz [1987]. Spatial chaos in the polarization for a birefringent optical fiber with periodic coupling, *Phys. Rev. Lett.* **58**, 1415-1418.

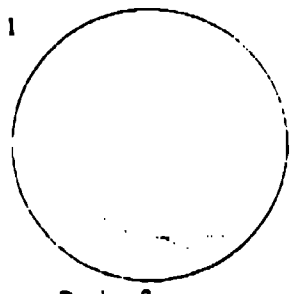
S. Wiggins [1988]. *Global Bifurcations and Chaos - Analytical Methods*, Springer-Verlag, New York.



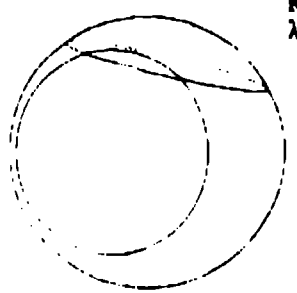
Region 1
 $\lambda = 1/2, \beta = 1$



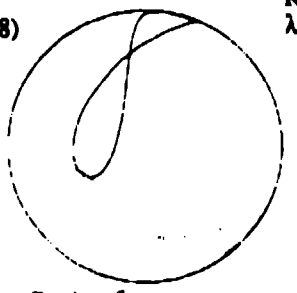
Region 2
 $\lambda = 0, \beta = \cos(\pi/8)$



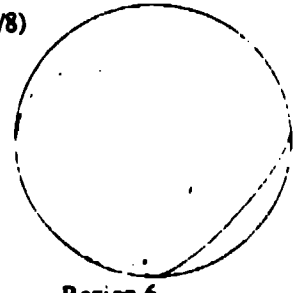
Region 3
 $\lambda = 1, \beta = \cos(\pi/8)$



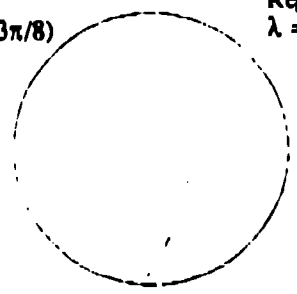
Region 4
 $\lambda = -1, \beta = \cos(3\pi/8)$



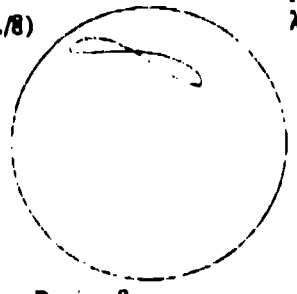
Region 5
 $\lambda = 1/2, \beta = \cos(3\pi/8)$



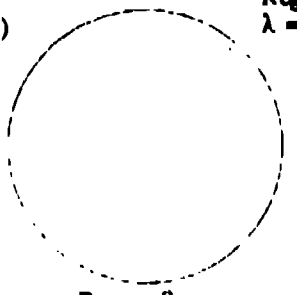
Region 6
 $\lambda = 2, \beta = \cos(3\pi/8)$



Region 7
 $\lambda = 0, \beta = \cos(7\pi/8)$



Region 8
 $\lambda = 1, \beta = \cos(7\pi/8)$



Region 9
 $\lambda = 1/2, \beta = -1$